Image-based Measurement of Changes to Skin Texture Using Piloerection for Emotion Estimation

Mihiro Uchida[1)] *, Rina Akaho[2)], Keiko Ogawa-Ochiai[3)], Norimichi Tsumura[4)]

1) Graduate School of Science and Engineering, Chiba University, 1-33, Yayoi-cho, Inage-ku, Chiba-shi, Chiba, 263-8522 Japan

2) Graduate School of Advanced Integration Science, Chiba University, 1-33, Yayoi-cho, Inage-ku, Chiba-shi, Chiba, 263-8522 Japan

3) Department of Japanese Traditional (Kampo) Medicine, Kanazawa University Hospital, 13-1 Takaramachi, Kanazawa-city, Ishikawa 920-8641, Japan

4) Graduate School of Engineering, Chiba University, 1-33, Yayoi-cho, Inage-ku, Chiba-shi, Chiba, 263-8522 Japan

*Email: mihiro.uchida@gmail.com

* Phone & Fax: +81-43-290-3262

Abstract: In this paper, we find effective feature values for skin texture as captured by a non-contact camera to monitor piloerection on the skin to estimate emotion. Piloerection is observed as goose bumps on the skin when a person is emotionally moved or scared. This phenomenon is caused by the contraction of the arrector pili muscles with the activation of the sympathetic nervous system. Piloerection changes skin texture, because of which we think it effective to examine skin texture to estimate the subject's emotions. Skin texture is important in the cosmetic industry to evaluate skin condition. Therefore, we thought that it will be effective to evaluate the condition of skin texture for emotion estimation. Evaluations were performed by extracting effective feature values from skin textures captured by using a high-resolution camera, where these feature values should be highly correlated with the degree of piloerection. The results showed that the feature value "the standard deviation of short-line inclination angles in texture" was satisfactorily correlated with the degree of piloerection.

Keywords: emotion estimation, goose bump, image processing, piloerection, skin texture

1 INTRODUCTION

Service robots are nowadays required to interact with humans more naturally in several domains of life. In such situations, the robots need to be capable of considering the customer's emotions to provide useful service. Some robots can recognize emotions through facial expression and speech recognition [1]. However, in many cases, they fail to recognize the emotions of a poker-faced person or one speaking in monotonous tones because they cannot detect emotional signals in these ways.

A large amount of research has been devoted to estimating emotions using biological information. For instance, it is possible to estimate emotions using an electroencephalogram [2] by attaching electrodes to subjects when measuring biological information. However, this process can be stressful for subjects. Moreover, robots can record information through non-contact methods that employ cameras and microphones. Okada et al. extracted pulse waves from sequential RGB images to estimate the emotions of subjects while watched stimuli in videos [3]. However, this method requires the designation of large regions of interest (ROI) and thus may fail to estimate the emotions of people with certain appearances, such as those with long bangs or wearing flu masks. Pulse waves may further not provide adequate information to estimate people's emotions in scenarios encountered in the service industry. Another method is thus needed to monitor emotions through non-contact methods.

As an interesting method to monitor emotions, the detection of piloerection has been used to research aesthetic chills [4]-[8]. However, the piloerection detection in the relevant studies was self-reported by the subjects. The task—observing their own arm—could have prevented them from concentrating on the stimuli and evincing intense emotions, and thus might have led to self-perception errors.

Sumpf et al. investigated the relationship between aesthetic chills and electrocardiogram (ECG) signatures using a Goose Cam, a device to auto-detect piloerection [9]. It consisted of a camera and light sources to capture images of the forearm [10]. However, the Goose Cam must be fixed to the subjects' arms for readings, which prevents the natural arousal of the intense emotions.

In this paper, we propose capturing skin textures in a non-contact manner to find effective feature values to monitor piloerection on the skin to estimate emotion. Piloerection is observed as goose bumps on the skin when

the subject is emotionally moved or scared. This phenomenon is caused by the contraction of the arrector pili muscles with the activation of the sympathetic nervous system, and changes skin texture. Due to piloerection, the skin around the pores protrudes from the surface. Figure 1 shows the typical skin texture, a pattern with a groove on the surface (called the sulcus cutis) and an area surrounded by it (called the crista cutis). In the cosmetics' industry, considerable research has been conducted to assess states of skin textures. For example, Takemae et al. built a system to evaluate skin condition by considering texture [11], and Kobayashi et al. built a system to assess the condition of the skin [12]. However, they obtained skin images using a contact method, which generated artifacts in their emotion analyses. They could thus only analyze long-term changes to skin texture, such as change caused by aging and differences in lifestyle. In this paper, we represent changes to skin texture using piloerection as a non-contact method by employing a high-resolution camera. This helps build an objective chill detection system. It also reduces the area of the ROI from images needed for emotion estimation.

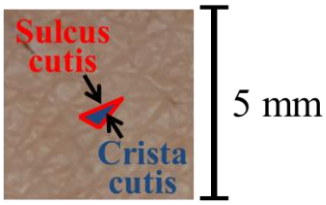

Fig. 1 Skin texture

2 PAST WORK [10]

In a previous study, the intensity of piloerection was objectively evaluated by image processing in the spatial frequency domain. It is known that the average density of hair follicles, the coats of hair in the skin, is 18 /cm^2 on the forearm [13]. In a previous paper, the maximum amplitude of a frequency range of approximately 18 /cm^2 was used to quantify piloerection intensity. The details of this process are described below.

Images obtained from a camera were modulated into 11 × 11 pixels capturing approximately a 1 × 1-mm area on the skin. The modulated images were then trimmed to 288 × 288 pixel images. The trimmed images were converted into grayscale images, and a high-pass filter was applied to the grayscale images with a cutoff at 4 cycles/picture. The purpose of this process was to eliminate skin curvature. A Two-dimensional discrete Fourier transform (2D DFT) was applied to the images to obtain images in the 2D frequency domain. Angular averaging was performed to obtain 1D frequency spectrum as directional information related to the components of frequency was not useful to calculate piloerection intensity in this method. Finally, piloerection intensity was obtained as the maximum amplitude in the range 6 ~ 20 cycles/picture at 1D frequency power. This method requires a large ROI to analyze many pores. In this study, we analyzed images of the skin using the method described in Section 3, as used in the cosmetics' industry [11]-[12].

3 METHODS

This section describes our method to analyze skin texture according to the flow shown in Fig. 2. The grayscale conversion described in Section 3.1 is first applied to the original images. The cross-binarization described in Section 3.2 is then applied to the grayscale images to clarify the sulci cutis [12], following which thinning is applied to obtain feature values with respect to skin texture [11]. This process is described in Section 3.3. The short-line matching described in Section 3.4 is also applied to the cross-binarized images to approximately express the sulci cutis as thin, short lines to obtain feature values with respect to skin texture [12]. Short-line matching detects sulci cutis and obtains feature values with respect to skin texture by assigning short, thin lines to each sulcus cutis expressed as black pixels in the cross-binarized image.

3.1 Grayscale conversion

We applied two grayscale conversion methods. One of the grayscale conversion is denoted by the following formula:

$$Y = 0.299R + 0.857G + 0.114B \quad (1)$$

where Y is the gray level; and R, G, and B are pixel values of the red, green, and blue channels, respectively. Changes

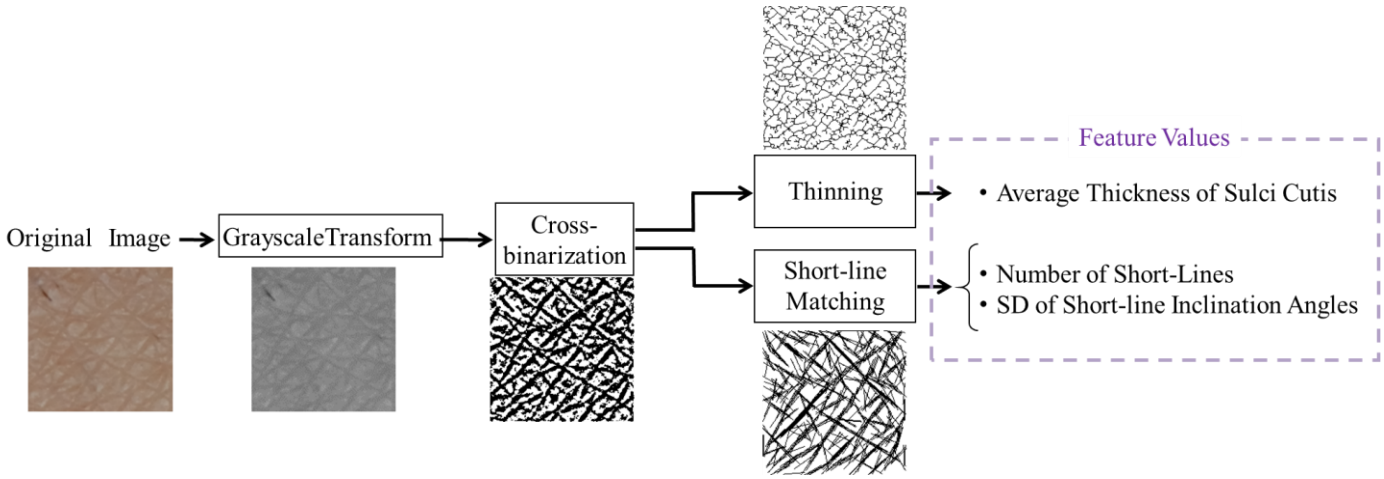

Fig. 2 The flow of our image processing method to extract the six feature values

in the color of the skin color change can occur due to changes in heartbeat and influence the feature values. For this reason, we obtained the L^* component of the CIELAB color space as another grayscale image. The L^* component is a luminance component that does not depend on RGB color. We then compare the feature values of the grayscale images based on RGB color space (denoted by the "*Y* component") with those of L^* (denoted by the "L^* component").

3.2 Cross-binarization [12]

Cross-binarization is a binarization that scans an image with a cross-shaped window of length *X* pixels, as shown in Fig. 3. It is used to clarify linear regions based on the difference between the gray level of the center pixel in the window and the average gray level of pixels in it excluding the center pixel. We chose the cross binarization because Otsu method [14] and the other binarization methods can be influenced by uneven illumination not to clarify sulci cutis. If the average gray level of the pixels minus the gray level of the center pixel is higher than a pre-determined threshold, denoted by *Th*, the pixel of interest is expressed as black. Otherwise, the pixel is expressed as white. This process can be denoted as following formula:

$$Interest = \begin{cases} 0 & (Ave - Center > Th) \\ 255 & (Ave - Center \le Th) \end{cases} \qquad (2)$$

where *Interest* is the gray level of the pixel of interest after binarized, *Ave* is the average gray level of pixels in it excluding the center pixel, *Center* is the gray level of the center pixel in the window, and *Th* is the threshold.

Two pre-determined parameters are needed for cross-binarization, the side length *X* and threshold *Th*. We empirically determined *X* as 19 and *Th* as zero in the experiment reported in Section 4. The result of cross-binarization is shown in Figs. 4 and 5, which represent the original and cross-binarized image, respectively.

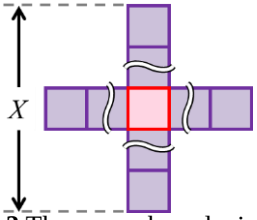

Fig. 3 The cross-shaped window

Fig. 4 The original image

Fig. 5 The cross-binarized image

3.3. Thinning

Thinning is first applied to the cross-binarized image described in Section 3.2, and Figure 6 shows the results of thinning. We can hence obtain the feature value—the average thickness of the sulci cutis—that is the ratio of the number of black pixels in the cross-binarized image to that in the thinned image.

3.4. Short-line matching [12]

The short-line matching is the process to detect sulci cutis by putting short thin lines on black pixels in the binarized image. We chose short-line matching because it can detect sulci cutis which have various lengths and widths without miss detection. The first and final states of short-line matching are shown in Fig. 7. To find a black pixel, the cross-binarized image described in Section 3.2 is first scanned for s pixels from top-left to right. If a black pixel is found, it is set as the start point. A short line of length *l* and width *h* is then drawn from the start point to the

right as shown in Fig. 7(a). If the ratio of the number of black pixels to the size of the short line is higher than γ%, the next short line is drawn from the end point of the last line along the same direction. Otherwise, it is drawn from the start point along the direction rotated by $\Delta\theta$. The step used to determine whether a match is obtained is repeated and the next short line drawn depending on the result. It is drawn along the same direction as the preceding line there is a match, and along the direction rotated by $\Delta\theta$ otherwise. After repeating this process until the short line to the left does not match, the direction along which most short lines are drawn is defined as the final direction relative to the start point, and the series of lines drawn along this direction is defined as the final line as shown in Fig. 7(b). It expresses a sulcus cutis. All pixels on the final line are then marked in order not to be used as start points in the following steps. Following this, the image is scanned again to find other start points. If the entire image is scanned, the short-line matching process is complete.

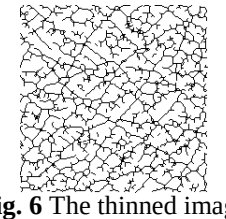

Fig. 6 The thinned image

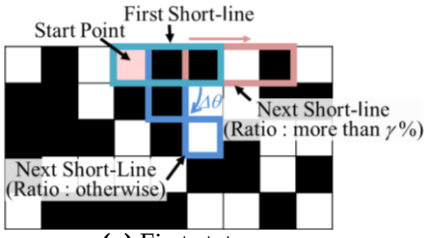

(a) First state

(b) Final state

Fig. 7 States of the short-line matching process

For short-line matching, five pre-determined parameters are needed: the length of the short lines (l pixels), their width (h pixels), the interval of the rotation angle ($\Delta\theta$ degrees), the scanning interval (s pixels), and the judgment border of matching (γ%). We empirically determined the parameter sets (l, h, $\Delta\theta$, s, γ) = (30, 1, 5, 2, 75) in the experiment reported in Section 4. The results of this process are shown in Fig. 7. The result of the application of short-line to the cross-binarized image shown in Fig. 5 is represented in Fig. 8. We obtained the following feature values with respect to skin texture using this process: *the number of short lines*, and *the standard deviation (SD) of their angles of inclination*. The number of short lines can help evaluate the area of the sulci cutis because each line has the same width and length. Also, the area of the sulci cutis is related to the thickness of sulci cutis because only the sulci cutis can change. The sulci cutis open and close as the skin stretches and shrinks [15]. These changes are expressed as getting thick and thin in the skin image. We expect the thickness of the sulci cutis changed by the geometry of the skin changing as piloerection evoking. The SD of the inclination angles of the lines expresses the variety of directions of the sulci cutis because each short line is placed along them. The variety of direction of sulci cutis is important to evaluate skin texture in cosmetic industry because sulci cutis on skin texture which looks good have much more various direction than sulci cutis on skin texture which looking bad. We assumed that the variety of direction of sulci cutis can be changed by piloerection because of skin geometry change.

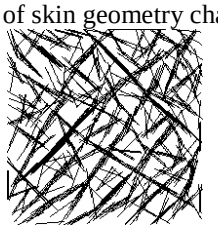

Fig. 8 The image after short-line matching

4 EXPERIMENT

In the experiment, we captured images of the surface of skin, where piloerection was invoked, once it began weakening. The images were analyzed by the image feature extraction introduced in Section 3.

4.1. Settings

Figure 9 shows our experimental settings. In a dim room, we remotely captured images of the skin on a subject's left forearm using a camera with a macro-lens. The working distance was 0.4 m and the subject's forearm was lit by two artificial sources of light. The resolution of the camera was 4928 × 3264 and the F number was 5.6. The shutter speed was 1/400 and ISO speed was 200. The room was set to a comfortable temperature for the subject, a 22-years-old female who could voluntarily get goose bumps.

4.2. Procedure

The participant was asked to invoke piloerection. Following this, images of the left forearm were captured for five seconds at intervals of one second. The participant placed her arm on a chin rest and grasped its pole, as shown in Fig.9.

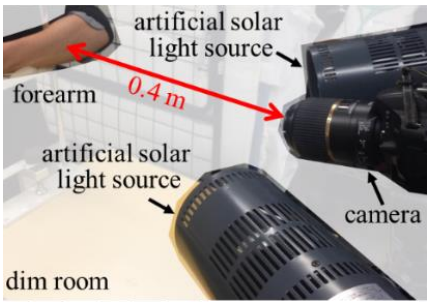

Fig. 9 The experimental setting

4.3. Obtaining skin images for analysis

The data were first saved as NEF files, which are raw data, and were converted into TIFF files (using Nikon View NX 2). To obtain 200 × 200-pixel images of the skin, which captured a 5 mm × 5 mm area, we manually trimmed all images based on visual marks to extract images of the skin at the same position. They were then analyzed using the image processing methods described in Section 3.

5 RESULTS

Fig. 10 shows images captured in the experiment described in Section 4. We can see that the piloerection weakened by observing visual changes in the images, where skin bulges around the pores are disappearing and the orientation of the hair appears to be changing.

The changes of feature values are shown in Fig.11. Figure 11(a) shows changes in the average thickness of the sulci cutis obtained using the thinning process described in Section 3.3. Figures 11 (b) and (c) show changes in the feature values yielded by skin texture analysis using the short-line matching described in Section 3.4. Figure 11(b) shows changes in the number of short lines and Figure 11(c) those in the SD of the inclination angles of the lines. The red lines show the results of the *Y* component and the blue lines show the results of the *L** component. The average thickness of the sulci cutis tended to increase as the goose bumps weakened, and that of the *L** component almost monotonically increased.

the *Y* component and the blue line those in the values of the *L** component. The number of short lines in both components tended to increase as piloerection weakened, whereas the SD of the inclination angles of the short lines of both components tended to decrease as piloerection weakened. In particular, the standard deviation of the inclination angles of the short lines of the *L** component was almost monotonically decreasing.

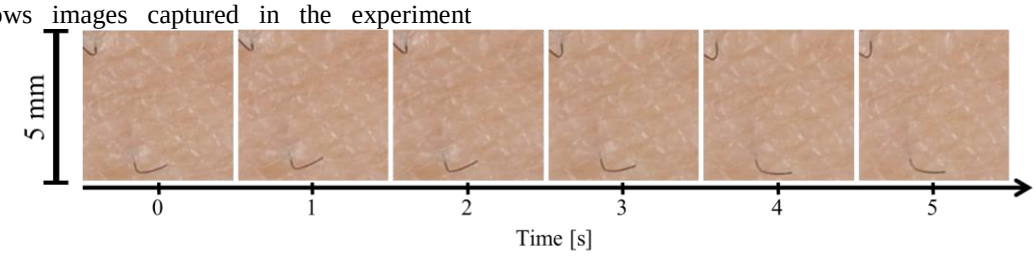

Fig. 10 Trimmed images captured in the experiment in Section 4

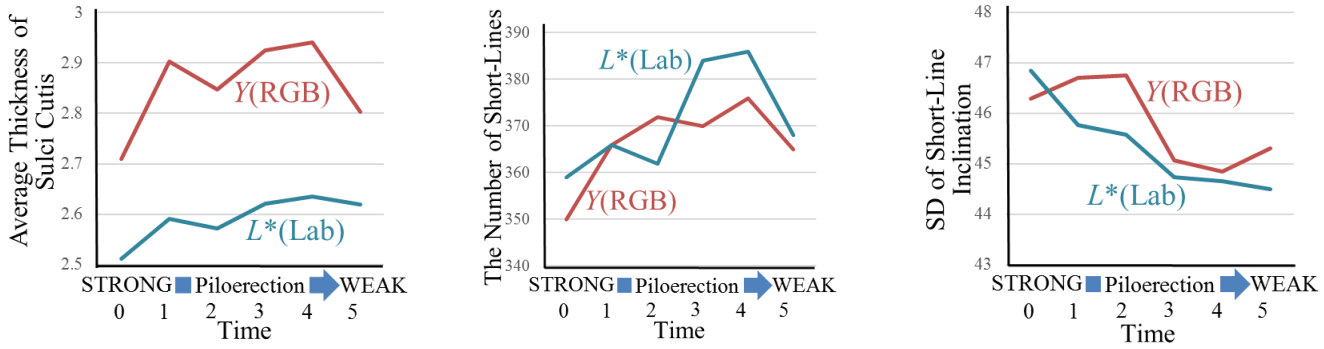

(a) Change in average thickness of sulci cutis

(b) Change in the number of short lines

(c) Change in the SD of short-line inclination angles

Fig. 11 Changes of each feature values as piloerection getting weak

6 DISCUSSIONS

It is said that piloerection voluntarily evoked shows the similar biological responses to piloerection naturally evoked such as increasing heart rate [4]. Therefore, in this study, we assumed that piloerection voluntarily evoked van be treat similarly to piloerection naturally evoked.

It is reasonable to expect that the thickness of sulci cutis changes because the skin stretches or shrinks as piloerection occurs. It is also reasonable to expect that the directions of sulci cutis are changed as the skin geometry changed by piloerection. Furthermore, the sulci cutis exist radially around the pores in the skin near the pores. Then, we analyzed very narrow area including two pores. Therefore, we consider that our findings can be general tendencies even if the degrees of changes are different among individuals. However, analyzing more samples is needed for further findings in our future work.

As mentioned in Section 5, the weaker the piloerection, the larger the average thickness of the sulci cutis of the L^* component, as shown in Fig. 11(a). Moreover, the weaker the piloerection, the smaller the SD of short lines of the L^* component, as shown in Fig. 11(c). Therefore, both are well-correlated with the degree of piloerection. Piloerection thins the sulci cutis and causes them to develop along various directions.

It is evident that color of the skin changed slightly as piloerection weakened, and this might have influenced the results. The skin with piloerection appeared reddish, whereas ordinary skin looked whitish in the images. In the former case, as the colors of the cristae cutis and the sulci cutis were similar, extracting the linear parts became challenging. This might have led to biases in binarization and changes in the feature values of the Y component. We can see in the Figs. 11 that the shapes of changes to each component are different.

A cause of changes in the color of the skin is a change in the volume of blood in the relevant area of the body. Piloerection is caused by the contraction of the erector pili muscles though the activation of the sympathetic nervous system, which also increases blood volume, and this causes the skin to look redder. The shading due to the bulges and the curvature of the skin are also thought to contribute to the change in skin color.

7 CONCLUSION AND FUTURE WORK

In this study, we analyzed changes to skin texture as piloerection weakened five seconds after inset. As the participant of our experiment had voluntarily invoked piloerection, we captured images of the skin of the left forearm at intervals one second. We confirmed that piloerection weakened by observing visual changes.

We obtained skin images for analysis by trimming entire images based on the mark which we draw on her arm. Grayscale conversion and cross-binarization were applied to the skin images to clarify shapes of the sulci cutis. Thinning was applied to the cross-binarized images to obtain a feature value, and short-line matching was used to obtain other feature values.

Changes in the average thickness of the sulci cutis were almost monotonically increasing as piloerection weakened. This suggests that piloerection thins the sulci cutis. On the contrary, changes to the standard deviation of the short-line inclination angles of L^* component were almost monotonically decreasing as piloerection weakened. This suggests that the sulci cutis, when piloerection is being invoked, are more varied in direction. These feature values can be used to express the degree of piloerection.

With regard to the structure of the skin, its 2D as well as 3D geometry changes with piloerection. Therefore, 3D texture analysis may provide useful feature values in analysis to yield further findings.

In this study, only one subject was analyzed. The trends of feature values may depend on the participant, because of which a wider-ranging experiment involving more people is needed in future work. Skin texture also varies between body parts, and thus different parts need to be studied in the future.

Emotion estimation should be robust against age, customs, and skin differences. However, skin texture depends on many of these variables. Therefore, both uniform skin texture and non-uniform skin textures need to be analyzed in the context of piloerection. Analyzing skins of various races is also useful for future research.

In this study, we analyzed only piloerection as physiological phenomenon. This needs to be applied to emotion estimation. Moreover, analyzing bio-information such as ECG and skin conductance can help reveal further relationships between piloerection and physiological response.

Our research here focused on skin texture and ignored other factors of the skin, such as pores, which can change owing to piloerection. Thus, an analysis of pores can help build a stable emotion estimation system using skin analysis.

ACKNOWLEDGMENT

We thank Saad Anis, PhD, from Edanz Group (www.edanzediting.com/ac) for editing a draft of this manuscript.

REFERENCES

[1] DailyMail, Pepper the 'emotional' robot sells out in ONE MINUTE: 1,000 models of the Japanese humanoid sell for $1,600 each, http://www.dailymail.co.uk/sciencetech/article-3134746/Pepper-emotional-robot-sells-ONE-MINUTE-1-000-models-Japanese-humanoid-sell-1-600-each.html (22 Nov 2017 accessed)

[2] Lin YP, Wang CH, Jung TP, et al (2010), EEG-Based Emotion Recognition in Music Listening, IEEE Transactions on Biomedical Engineering 57(7): 1798-1806

[3] Okada G, Kurita K, Yonezawa T, et al (2018), Monitoring Emotion by Remote Measurement of Physiological Signals Using an RGB Camera, ITE Transactions on Media Technology and Applications, 6(1): 131-137.

[4] Lndsley DB, and Sassaman, WH (1938). Autonomic activity and brain potentials associated with" voluntary" control of the pilomotors (Mm. arrectores pilorum). Journal of Neurophysiology, 1(4): 342-349.

[5] Rickard NS (2004), Intense emotional responses to music: a test of the physiological arousal hypothesis, Psychology of Music 32(4):371-338

[6] Panksepp J (1995), The emotional sources of “chills” introduced by music, Music Perception 13(2):171-207

[7] Blood AJ, Zatorre RJ (2001), Intensely pleasurable responses to music correlate with activity in brain regions implicated in reward and emotion, Proceeding of the National Academy of Sciences 98(20):11818-11823

[8] Guhn M, Ham A, Zenter M (2005), Physiological and musico-acoustic correlates of the chill-response, Music Perception 24(5):473-483

[9] Sumpf M, Jentschke S, Koelsch S (2015), Effects of Aesthetic Chills on a Cardiac Signature of Emotionality, PLoS ONE 10(6): e0130117

[10] Benedek M, Wilfing B, Lukas-Wolfbauer R (2010), Objective and continuous measurement of piloerection, Psychophysiology 2010 Sep 47(5):989-993

[11] Takemae Y, Saito H, Ozawa S (2001), The Evaluating System of Human Skin Surface Condition by Image Processing, Transactions of the Society of Instrument and Control Engineers, 37(11): 1097-1103 (In Japanese)

[12] Kobayashi H, Hashimoto T, Yamazaki K, et al (2010), Proposal of quantitative index of skin texture by the image processing and its practical application, Transactions of the Japan Society of Mechanical Engineers, Part C, 76(764), 922-929. (In Japanese)

[13] Otberg N, Richer H, Blume-Peytavi U, et al (2004), Variations of hair follicle size and distribution in different body sites, Journal of Investigative Dermatology, 122(1), 14-19.

[14] Otsu N (1979), A threshold selection method from gray-level histograms, IEEE Transaction on Systems, Man, and Cybernetics. 9(1): 62–66.

[15] Shiseido, Elucidating the relationship between beautiful texture and elastic fiber "Oxitalan fiber" - At the same time, developing corresponding ingredients that nurture fine and well-shaped texture -, https://www.shiseidogroup.jp/releimg/1900-j.pdf (26 Apr 2018 accessed) (In Japanese)